PROCEEDINGS OF SPIE

SPIEDigitalLibrary.org/conference-proceedings-of-spie

Calibration-free technique for the measurement of oxygen saturation changes in muscles of marine mammals and its proof of concept

Antonio Ortega-Martinez, Chhavi Goenka, Marloes Booker, Robert M. H. Grange, Allyson G. Hindle, et al.

Antonio Ortega-Martinez, Chhavi Goenka, Marloes Booker, Robert M. H. Grange, Allyson G. Hindle, Walfre Franco, "Calibration-free technique for the measurement of oxygen saturation changes in muscles of marine mammals and its proof of concept," Proc. SPIE 10489, Optical Biopsy XVI: Toward Real-Time Spectroscopic Imaging and Diagnosis, 104890D (19 February 2018); doi: 10.1117/12.2290546



Event: SPIE BiOS, 2018, San Francisco, California, United States

Calibration-free technique for the measurement of oxygen saturation changes in muscles of marine mammals and its proof of concept

Antonio Ortega-Martinez^{a,b}, Chhavi Goenka^{a,b}, Marloes Booker^c, Robert M. H. Grange^d, Allyson G. Hindle^d, Walfre Franco^{a,b,*}

^aWellman Center for Photomedicine, Massachusetts General Hospital, Boston, MA, USA
 ^bDepartment of Dermatology, Harvard Medical School, Boston, MA, USA
 ^c Department of Physics, Xavier University of Louisiana, New Orleans, Louisiana, USA
 ^dAnesthesia Center for Critical Care Research, Department of Anesthesia, Critical Care and Pain Medicine, Massachusetts General Hospital, Harvard Medical School, Boston, MA, USA

ABSTRACT

Marine mammals possess impressive breath-holding capabilities made possible by physiological adjustments during dives. Studying marine mammals in their natural environment unravels vital information about these physiological adjustments particularly when we can monitor altered dive behavior in response to stressful situations such as human-induced oceanic disturbances, presence of predators and altered prey distributions. An important indicator of physiological status during submergence is the change in oxygen saturation in the muscles and blood of these mammals. In this work, we aim to investigate oxygen storage and consumption in the muscles of free-diving elephant seals when exposed to disturbances such as sonar or predator sounds while they are at sea. Optical oxygen sensors are a mature technology with multiple medical applications that provide a way to measure oxygenation changes in biological tissues in a minimally invasive manner. While these sensors are well calibrated and readily available for humans, they are still inadequate for marine mammals primarily due to a very small number of test candidates and therefore little data is available for validation and calibration. We propose a probe geometry and associated mathematical model for measuring muscle oxygenation in seals based on near infrared diffuse transport with no need for calibration. A prototype based on this concept has been designed and tested on humans and rats. We use the test results to discuss the advantages and limitations of the approach. We also detail the constraints on size, sensor location, electronics, light source properties and detector characteristics posed by the unique biology of seals.

1. INTRODUCTION

Marine mammals such as seals and sea lions are top predators in ocean ecosystems that pursue their prey to depth but must return to the surface to breathe. These species have highly specialized cardiovascular physiology that enables them to extend submergence time, by altering their heart rate and perfusion of tissues. They also draw down body oxygen stores during extended dives [1] exposing their tissues to hypoxia and to ischemia/reperfusions events. For example, diving Northern elephant seals (*Mirounga angustirostris*) appear able to consume all available oxygen during long dives, surfacing with a nearly depleted venous reserve [2]. This extreme physiology may, on one hand, provide key medical insights for human interventions to treat hypoxic events (e.g. myocardial infarction, stroke, hemorrhage, sepsis). At the same time, it is clear that physiology imposes a species-specific limit on diving capacity for marine mammals in their natural environment, and is likely a limiting factor in their ability to alter diving in response to disturbance.

Ocean habitats are increasingly disrupted by human activities and habitat change. Many marine mammals react to disturbance by changing their diving behavior, however the cost of these adjustments and the extent to which physiological thresholds limit the scope of behavioral responses is unknown. In order to achieve an integrated understanding of oxygen management and hypoxia tolerance in diving seals that can be applied to human medicine, as well as to determine the resilience of marine mammals to disruption, it is necessary to monitor physiology of freely diving animals under routine conditions and in response to

*Send correspondence to W.F. Email: wfranco@mgh.harvard.edu

Optical Biopsy XVI: Toward Real-Time Spectroscopic Imaging and Diagnosis, edited by Robert R. Alfano, Stavros G. Demos Proc. of SPIE Vol. 10489, 104890D ⋅ © 2018 SPIE ⋅ CCC code: 0277-786X/18/\$18 ⋅ doi: 10.1117/12.2290546

disturbance. Commercially available technologies to measure intravascular oxygen tensions via a Clark electrode are difficult to source but have been modified for use in unrestrained diving vertebrates [2,3] Two first-generation, purpose-built devices have also been surgically placed to measure muscle myoglobin saturation in diving seals and penguins with near-infrared spectrometry [4,5]. As part of a larger project to measure the integrated physiological and behavioral responses of Northern elephant seals to at-sea experimental disturbance, here we present a prototype of a second-generation, low cost calibration-free probe to measure muscle oxygen in marine mammals based on near infrared diffuse transport. Measurements from this removable probe, placed on the muscle with a short-term implantation procedure will allow us for the first time to develop a model of oxygen use in swimming muscle of elephant seals (with and without disturbance), and to model the transfer of oxygen between blood and muscle.

Elephant seals are an ideal model for teasing apart cardiovascular physiology from local tissue (muscle) strategies to manage oxygen stores and their response to disturbance, because: 1) this species is well-studied, providing an important baseline level of biological information; 2) they have excellent underwater hearing [6] making them sensitive to acoustic disturbances [7]; 3) they are deep, long duration divers that exhibit exceptional hypoxia tolerance [2]; 4) they are easily accessible and they tolerate instrumentation well [8]; 5) they will return to the same beach after being translocated, facilitating attachment and retrieval of biologgers [9].

In order to study physiology of unrestrained seals diving in the open ocean, instruments must be neutrally buoyant in seawater and small enough in size/shape to not disrupt the animal's hydrodynamics. Dataloggers and control units must also be contained in pressure-proof, watertight housings, and temporarily glued to the seal's fur, for easy removal after several days of diving when the seal returns to the beach. As optical data on marine mammals is sparse, very little calibration information exists, and therefore the measurement technique must be calibration free. A calibration-free measurement also makes this second-generation instrument minimally invasive, as it does not require the surgical removal of a large muscle piece for post-deployment calibration. Optical instruments using modulated light sources have been proposed to measure oxygen saturation. However, they employ phase detection techniques [10,11] that require expensive and sophisticated equipment that is not easily miniaturized for field tests on marine mammals.

In this work, we propose the concept and design of a probe that uses amplitude detection to measure oxygen saturation. Section 2 discusses the mathematical methodology to obtain oxygen saturation from amplitude measurement of the modulation signal. The design of the probe and associated hardware is detailed in Section 3. Section 4 discusses the results obtained during preliminary tests and Section 5 explains the challenges posed by the requirements on the design and the future work that will be required in order to field test the final device.

2. MATHEMATICAL MODEL

2.1 Diffuse model

When light travels through highly scattering media, such as tissues, photons experience random changes in direction. If a light source is placed in contact with the surface of a scattering medium, a portion of the light will be backscattered and returned back to the input surface, creating a spot or distribution of light around the source [12]. The shape of this spot is dependent on the optical properties of the tissue. As many biological tissues are highly scattering, extensive research has been carried out to obtain a mathematical model for the backscattered light distribution around the source under various assumptions. For the case of a semi infinite medium in which the scattering coefficient is much higher than the absorption coefficient illuminated with a sinusoidally modulated light source, the light distribution on the surface as a function of the distance to the source ρ [13,14] is given by

$$U_{AC}(\rho) = \frac{SA}{4\pi\rho vD} e^{-\rho\cos\left(\frac{1}{2}atan2(\omega, v\mu_a)\right)\left(\frac{(v\mu_a)^2 + \omega^2}{(vD)^2}\right)^{1/4}}$$
(1)

where S is the number of photons per second leaving the source, A is the AC amplitude of the modulation, μ_a is the absorption coefficient of the medium, ν is the speed of light in the medium, ω is the angular modulation frequency and D is the mean collision distance defined as one third of the reciprocal of the sum of the absorption and reduced scattering coefficients.

If the modulation frequency is much lower than the product $\nu\mu_a$, equation 1 gets simplified to $U_{AC}(\rho) = \frac{3\mu_S'SA}{4\pi\rho\nu c}e^{-\rho\sqrt{3\mu_a\mu_S'}}$ (2)

$$U_{AC}(\rho) = \frac{3\mu_{S}'SA}{4\pi\alpha\nu_{C}}e^{-\rho\sqrt{3\mu_{a}\mu_{S}'}}$$
(2)

where μ_s is the scattering coefficient

2.2 Self referenced calculation of oxygen saturation using AC amplitude

Calibration-free methods for calculating oxygen saturation have been suggested by other authors. These use AC phase detection on a backscattering setup. While phase detection methods have high accuracy, they often require expensive equipment and high frequencies. Since these requirements cannot be fulfilled while designing a low-cost autonomous device that uses the approximation presented by equation 2 (and hence, low modulation frequencies), we propose an alternate approach based on the measurement of AC amplitude instead of phase.

Equation 1 is dependent not just on the distance of detector from source, ρ , but also on the wavelength of the source, λ . Making this dependence explicit, equation 2 can be rewritten as

$$U_{AC}(\rho,\lambda) = \frac{3\mu_s'(\lambda)n(\lambda)S(\lambda)A}{4\pi\rho c}e^{-r\sqrt{3\mu_a(\lambda)\mu_s'(\lambda)}}$$
(3)

Thus, $U_{AC}(\rho_1,\lambda_1)$ is the AC amplitude at a distance ρ_1 and wavelength λ_1 .

According to Fantini et al [13] and Chance et al [11] the ratio, R, of absorption coefficients, μ_{a1} and μ_{a2} , at two different wavelengths, can be used to calculate the oxygenation, Y, under certain assumptions. To obtain this ratio, we make four measurements: measurements at two wavelengths, λ_1 and λ_2 at one source-todetector distance ρ_1 and at the same wavelengths at detector distance ρ_2 .

We can take the ratio of the two measurements at distances ρ_1 and ρ_2 , at the same wavelength λ_1 , and obtain

$$\frac{U_{AC}(r_1, \lambda_1)}{U_{AC}(r_2, \lambda_1)} = \frac{r_2}{r_1} e^{(r_2 - r_1)\sqrt{3\mu_a(\lambda_1)\mu_S'(\lambda_1)}}$$
(4)

Taking the natural logarithm, we get

$$\ln\left(\frac{U_{AC}(r_1,\lambda_1)}{U_{AC}(r_2,\lambda_1)}\frac{r_1}{r_2}\right) = (r_2 - r_1)\sqrt{3\mu_a(\lambda_1)\mu_s'(\lambda_1)}$$
 (5)

Repeating the equations 4 and 5 for measurements at distances ρ_1 and ρ_2 , at wavelength λ_2 , and then taking the ratio, we obtain

$$\frac{\ln\left(\frac{U_{AC}(r_1,\lambda_1)}{U_{AC}(r_2,\lambda_1)}\frac{r_1}{r_2}\right)}{\ln\left(\frac{U_{AC}(r_1,\lambda_2)}{U_{AC}(r_2,\lambda_2)}\frac{r_1}{r_2}\right)} = \frac{\sqrt{\mu_a(\lambda_1)\mu_s'(\lambda_1)}}{\sqrt{\mu_a(\lambda_2)\mu_s'(\lambda_2)}}$$
(6)

From here we can use the approach proposed by Fantini et al [7] and Chance et al [5] and calculate the ratio of the absorption coefficients as

$$R = \frac{\mu_a(\lambda_1)}{\mu_a(\lambda_2)} = \frac{\mu_s'(\lambda_2)}{\mu_s'(\lambda_1)} \left(\frac{\ln\left(\frac{U_{AC}(r_1, \lambda_1)}{U_{AC}(r_2, \lambda_1)} \frac{r_1}{r_2}\right)}{\ln\left(\frac{U_{AC}(r_1, \lambda_2)}{U_{AC}(r_2, \lambda_2)} \frac{r_1}{r_2}\right)} \right)^2$$
(7)

This can then be used to calculate the oxygenation Y given by Fantini as

$$Y = \frac{B_1 - RB_2}{B_1 - O_1} \tag{8}$$

3. PROTOTYPE DESIGN

The oxygen sensor consists of two parts: the control electronics and the optical probe. The current prototype uses a 3D printed black thermoplastic probe. The probe comprises the light sources and the detector. Three multiwavelength LEDs (L660/735/805/940-40B42-C-I, Marubeni, Santa Clara, CA) serve as the light sources and the detector is a monolithic chip containing a photodiode and transimpedence amplifier (Opt101, Texas Instruments, Dallas, TX). Figure 1 shows a block diagram of the prototype.

To implement the mathematical model proposed in the previous section, the probe only requires LEDs at two different distances from the sensor but the probe was implemented with three LEDs at three distances to enable us to do additional tests to correlate signal quality with distance. Each of the three LEDs has four wavelengths available: 660, 735, 805 and 940 nm. However, only 660 and 805 nm wavelengths were wired as they are the only ones being used. The additional wavelengths are there in case additional tests with other wavelengths are desired in the future. The center-to-center distances from the photodiode to the center of three LEDs are 0.85, 1.53 and 2.19 cm, which we will call ρ1, ρ2 and ρ3, respectively.

The probe is wired to the control electronics with a ten-wire ribbon cable. These control electronics comprise an oscillator, a magnitude detector, a microprocessor, an Arduino Uno board and current sources for the LEDs. In addition to this, there is also an SD card for data storage. The microprocessor (Atmega8, Atmel, San Jose, CA) provides the control signal and the analog to digital conversion of the sensor signal. It is programmed using the Arduino Uno board (Arduino R.I., Scarmagno, Italy) and provides time enabled signals for the LEDs. The LEDs are alternatively turned on in the following sequence: 660 nm at $\rho 1$ (where $\rho 1$ is the distance 1, 0.85 cm), 805 nm at $\rho 1$, 660 nm at $\rho 2$, 805 nm at $\rho 2$, 805 nm at $\rho 3$ and 805 nm at $\rho 3$.

When the LEDs are on, a quadrature oscillator sinusoidally modulates them at 5 kHz. The oscillator output is sent to voltage-to-current amplifiers. Each LED has its own amplifier each with a different gain. The irradiated power of these LEDs is approximately 150 μ W/mA. The appropriate current levels were determined with preliminary tests on phantoms simulating known tissue optical properties and on the skin of healthy human volunteers. LEDs farther away from the photodetector have higher gain in order to compensate for the exponential decay the light experiences when traveling through the tissue. The amplitude of the AC current is 20 mA for the LEDs at distance ρ 3. The AC has a 40 mA offset so the LED is always on and the sine wave is not rectified by the diode. The LEDs at distance ρ 3 were not used for animal validation tests due to their low signal quality in preliminary tests.

The signal measured by the photodiode is sent to a logarithmic magnitude detector, where it is compared with a reference signal, i.e. the oscillator input, and the resulting signal is digitized by one of the Atmega analog-to-digital converters. The signal is then stored on the SD card. The relative light intensity is stored along with the time of capture and the identifying name of the LED that was acting as the source at the time of capture.

4. RESULTS

4.1 Human Model

The prototype was tested on a simple human model to prove the concept of using amplitude change in order to measure oxygen saturation in blood. The probe was placed on the underside of the forearm of a volunteer, being careful to not have it over veins or moles. A pressure cuff was placed on the same arm. The baseline oxygen saturation was monitored with the probe. Then air is pumped into the cuff to apply pressure to the arm. The pressure is maintained at the 180-220 mg range for one minute and then released. Due to the higher oxygen consumption by the tissue and reduced blood flow, the oxygen saturation is expected to go down during the high-pressure period. The oxygen saturation is expected to slowly increase over baseline as the pressure is released due to the overcompensating influx of blood.

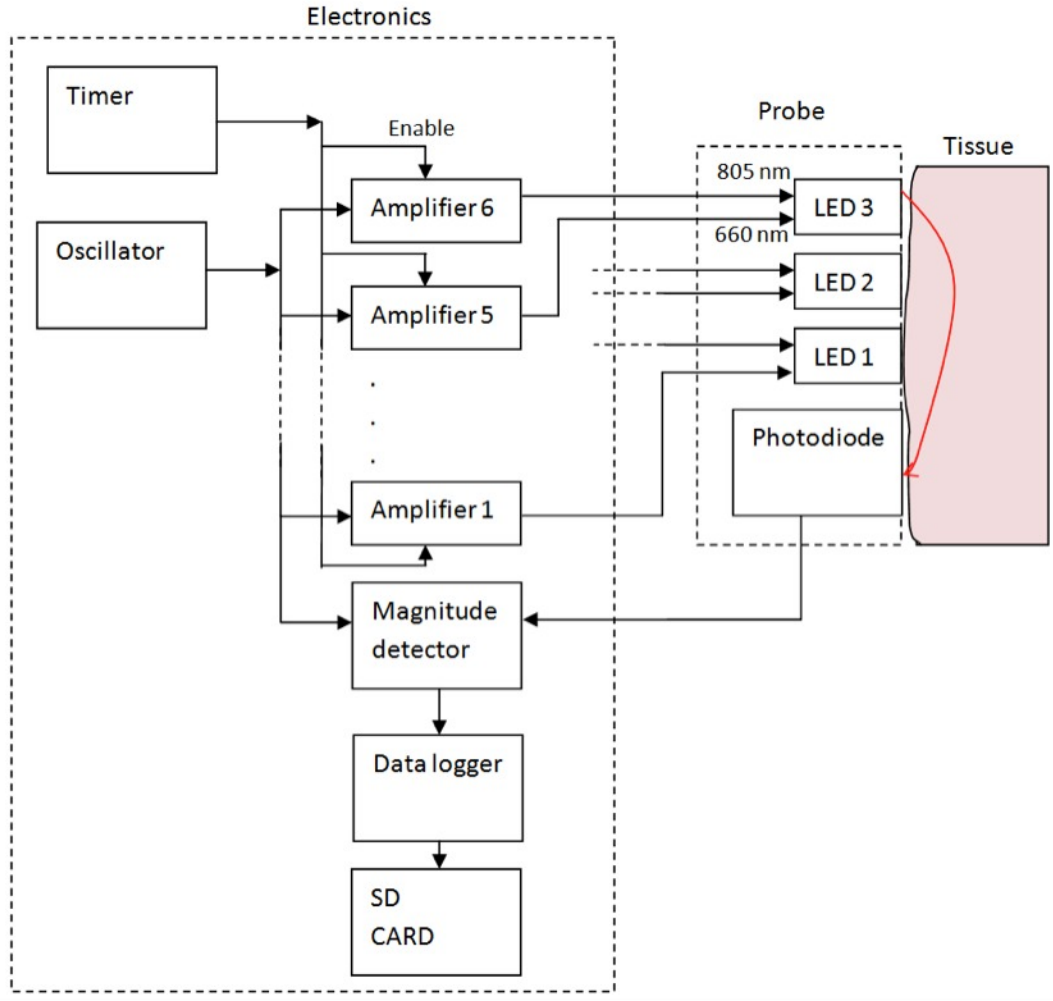


Figure 1: Block diagram of the prototype

The results for this test were within the expected values. Before applying pressure to the cuff (baseline), the median was 80%. Approximately 30 seconds after we start applying pressure (while the pressure is still on), the median oxygen saturation is 75%. After releasing the pressure, the oxygen saturation climbs to 87%, which is a median value.

4.2 Animal Model

An animal model was also used to test the probe's ability to measure changes in tissue oxygenation during an experimental hypoxia exposure, by validating muscle oxygen saturation levels versus arterial blood. We used a rat as the animal model. The rat was anesthetized with inhaled isoflurane, and could be exposed to varied levels of inspired oxygen via a nose cone (and therefore could receive controlled, varied exposure to hypoxia). Arterial oxygen saturation was measured continuously using a pulse oximeter (MouseOx). To measure the saturation of muscle myoglobin, we placed the probe directly onto the hindlimb muscle fascia. To do this, we applied local analgesia, then excised the skin and exposed the muscle surface with careful blunt dissection to avoid tissue trauma or disrupted blood vessels. Baseline data was collected while the rat breathed normoxic air (21% O₂). Hypoxia was then induced by altering the nitrogen content of inspired air to achieve 11% O₂. Stable arterial and muscle oxygen saturations were observed after ~15 min hypoxia in the rat (Fig. 2), following which, normoxia was restored. All animal procedures conformed to ethical guidelines and were approved by Institutional IACUCs and appropriate federal permits.

Our results conformed to the expected physiological response to hypoxia, with a rapid decline in arterial saturation, but a delayed, reduced drop in muscle oxygen saturation. The discrepancy in desaturation between the two respiratory pigments is explained by the higher O₂-affinity of myoglobin over hemoglobin, that allows muscle to sequester and strip oxygen carried by blood. The result is a tightly guarded store of muscle oxygen that can take minutes to consume. Indeed, even after 15 min of hypoxia, muscle oxygen saturation continues to slowly decline (Fig. 2). We also observed a similar short-term saturation increase for both blood and muscle to levels higher than baseline, once normoxia was restored, with these values eventually resolving to baseline levels.

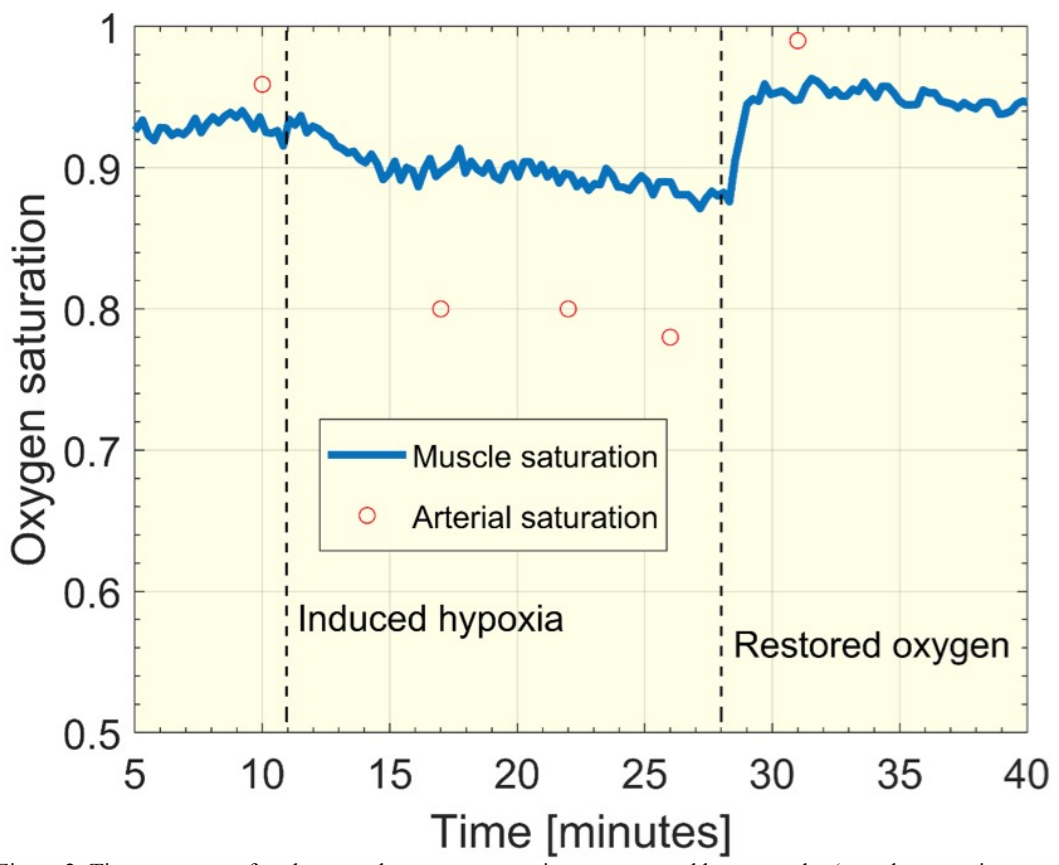


Figure 2: Time response of rat leg muscle oxygen saturation as measured by our probe (muscle saturation, continuous line), compared with pulse oximetry data (circles). Changes in oxygen content of inspired air are indicated by vertical lines (Hypoxia: 11% O₂, Baseline/Restored oxygen: 21% O₂).

To investigate the potential confounding effect of vascularization in our muscle preparation, we repeated this experiment, but placed the probe directly above the femoral artery. We confirmed that a signal from blood likely does confound the measurement of muscle saturation – in this preparation, oxygen saturation declined rapidly to <80%, where it remained stable, which is consistent with the results recorded in the blood during the initial hypoxia exposure (Figs. 2, 3).

5. DISCUSSION

5.1 Validity of approximation

As this probe is designed to be surgically implanted on the muscle surface directly, the model used to derive these equations does not include the skin. While this is not a problem for the intended target, it is a source of error for the proof of concept on humans. However, the ratio calculations tend to compensate for melanin.

The LEDs on the probe have a diameter comparable to the size of the rat muscle and larger than the artery. Due to this, the medium is not well approximated by a homogeneous medium, and we expect the measurements to contain contributions from different types of tissue at different layers. In the case of the experiment on the artery, this means that some of the light that reaches the detector traveled through the artery, but some light did not. We expect these results to be an average of different tissues, including some that have not been included in the model, e.g. bone. Still the results show agreement with the expectation. The homogenous medium approximation is expected to hold better in the case of elephant seals whose muscles are larger.

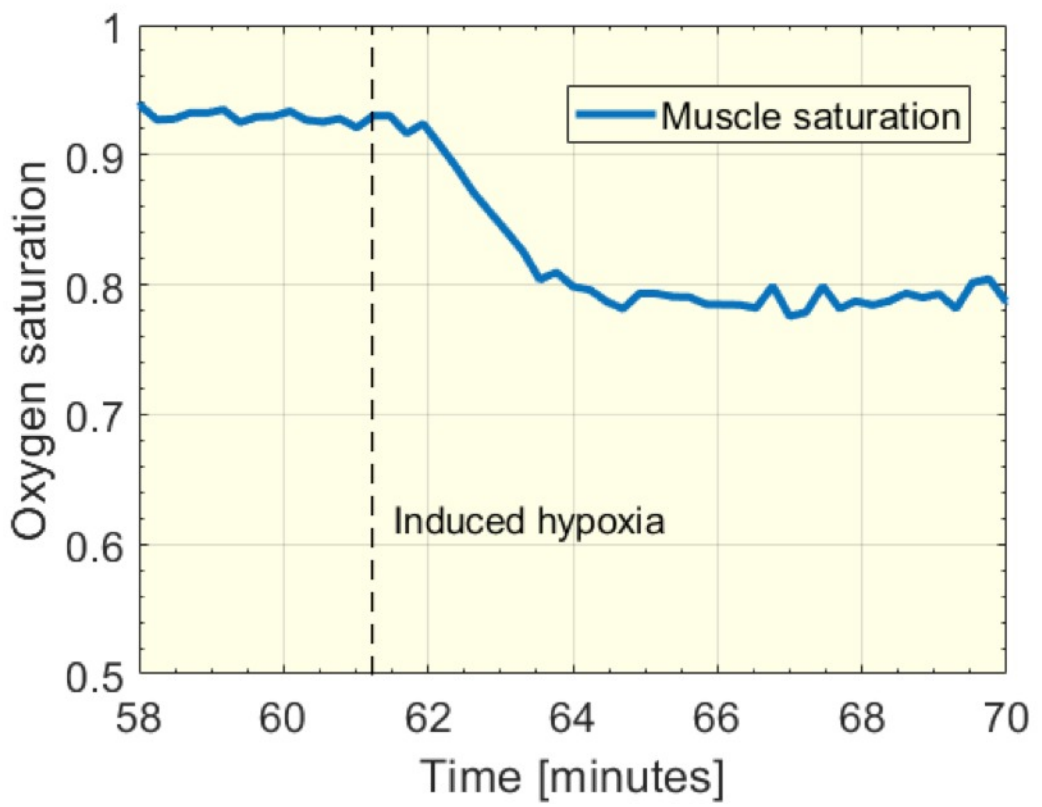


Figure 3: Time response of rat leg muscle oxygen saturation as measured by our probe, when the probe is placed on top of an artery. Change in oxygen content of inspired air is indicated by the vertical line (Induced hypoxia: 11% O₂).

5.2 Error estimation

The primary task of the proposed instrument is to measure muscle saturation. Even though muscle saturation is related to arterial saturation, they are not equivalent. Primarily, differences in these metrics are due to the kinetic and O₂-affinity differences between respiratory pigments (tetrameric hemoglobin in blood versus monomeric muscle myoglobin), as well as the result of variation in muscle perfusion, which infuses the tissue with arterial O₂-carrying blood, under different physiological conditions. While the sensor is self-calibrated, it is expected that the measurements will deviate from the real values. It is challenging to estimate this deviation since most commercial devices are designed for measuring arterial saturation.

5.3 Power consumption of device

The power consumption of the device is variable depending on which part of the measurement cycle is running, i.e. which LED is acting as the source. Usually, the maximum power consumption is when data is being written on the SD card (500 mW), and lower when all LEDs are off (50 mW). Using an electric power meter, on average the power consumption was 300 mW (60 mA current draw). A common USB 5V battery pack with a capacity of 2000 mAh contains enough energy to power the device for 33 hours. The final power

consumption would also depend on number of measurements per minute. Currently, the probe is programmed to turn each LED on for more than one second at a time in order to make debugging and testing easier, but in the final application it is only necessary to have them on for a shorter time. Also, while in the current prototype measurements are taken back to back (another cycle starts the moment the previous cycle finishes), this is not necessary in the final application, where one measurement per minute might be enough. Under those conditions, the power consumption of the device would be lower, enabling the device to be autonomous. Higher capacity batteries exist, but they are heavier and the weight of the prototype is required to be as low as possible.

5.4 Challenges due to seal muscle color and thickness

A prototype was tested on an anesthetized elephant seal. The objective of this test was to understand the depth of the incision necessary to implant the probe in the animal and to measure the signal levels obtainable. No hypoxia was induced during this test. A hallmark of diving mammals is enhanced body oxygen stores, a significant portion of which are carried in blood and muscle [1]. Therefore, the color of seal muscle, which is significantly darker than a human or rat muscle due to high myoglobin content, posed the most significant challenge. As the light travels through the muscle before reaching the detector, the signals obtained were very low. More tests on seal muscle will be done to figure out the appropriate source intensity to get measurable signal at the detector.

5.5 Future work

This device will support a large-scale field project investigating cardiovascular and behavioral responses of translocated, freely diving elephant seals. Muscle oxygen saturation is a key indicator of exercise capacity, hypoxia tolerance, control of circulation, and whole-body metabolic rate. Our ultimate goal is to couple muscle oxygen saturation, measured by this device and recorded via a data logger secured in a pressure-tested underwater housing, with dive behavior (depth and speed), electrocardiogram (EKG) and blood oxygen levels in routine dives versus dives with experimental acoustic disturbance.

The requirements posed on the device for this application are low weight and small size. To achieve this, certain hardware changes will be made to the device. The current prototype is built on two breadboards using mostly through-hole components. The final device will be implemented on a printed circuit board using surface mount components. The probe will be made smaller and flatter by using smaller LEDs in the next version of the design.

6. CONCLUSION

The experiments and results discussed here show that it is possible to make measurements of oxygen saturation changes with a probe that is portable and self-referenced, avoiding the necessity for calibration for non-human animals, whose optical properties might be unknown. The technique results in a low cost and convenient measurement of relative oxygenation changes. Further development of the device would involve its implementation on a printed circuit board and an optimization of its emitted power in order for it to work optimally on the elephant seals.

7. ACKNOWLEDGEMENTS

This work was supported by a grant from NSF IOS-1656077 to A. Hindle and W. Franco. We gratefully acknowledge Drs. B. McDonald, C. Williams, P. Ponganis, and D. Costa who facilitated the elephant seal pilot experiment, as well R. Holser and L. Huckstadt for field support. W. Franco gratefully acknowledges the financial support of Dr. R. Rox Anderson.

8. REFERENCES

- [1] Ponganis PJ, Meir JU, Williams CL. In pursuit of Irving and Scholander: a review of oxygen store management in seals and penguins. *J Exp Biol*. 2011;214(Pt 20):3325-39. doi:10.1242/jeb.031252.
- [2] Meir JU, Champagne CD, Costa DP, Williams CL, Ponganis PJ. Extreme hypoxemic tolerance and blood oxygen depletion in diving elephant seals. *Am J Physiol Regul Integr Comp Physiol*. 2009;297(4):R927-39. doi:10.1152/ajpregu.00247.2009
- [3] McDonald BI, Ponganis PJ. Insights from venous oxygen profiles: oxygen utilization and management in diving California sea lions. The Journal of experimental biology. 2013;216(17):3332-41
- [4] Guyton GP, Stanek KS, Schneider RC, et al. Myoglobin saturation in free-diving Weddell seals. *J Appl Physiol*. 1995;79(4):1148-1155.
- [5] Williams CL, Meir JU, Ponganis PJ. What triggers the aerobic dive limit? Patterns of muscle oxygen depletion during dives of emperor penguins. *J Exp Biol.* 2011;214(Pt 11):1802-1812. doi:10.1242/jeb.052233.
- [6] Kastak, D. & Schusterman, R. J. In-air and underwater hearing sensitivity of a northern elephant seal (*Mirounga angustirostris*). *Can J Zool* 77, 1751-1758 (1999).
- [7] Fregosi, S., Klinck, H., Horning, M., Costa, D. P., Mann, D., Sexton, K., Hückstädt, L. A., Mellinger, D. K. & Southall, B. L. An animal-borne active acoustic tag for minimally invasive behavioral response studies on marine mammals. *Animal Biotelemetry* 4:9, doi:10.1186/s40317-016-0101-z (2016).
- [8] McMahon, C. R., Field, I. C., Bradshaw, C. J., White, G. C. & Hindell, M. A. Tracking and data—logging devices attached to elephant seals do not affect individual mass gain or survival. *J Exp Mar Biol Ecol* 360, 71-77 (2008).
- [9] Andrews, R. D., Jones, D. R., Williams, J. D., Thorson, P. H., Oliver, G. W., Costa, D. P. & LeBoeuf, B. J. Heart rates of northern elephant seals diving at sea and resting on the beach. *J Exp Biol* 200, 2083-2095 (1997).
- [10] Sevick EM, Chance B, Leigh J, Nioka S, Maris M. Quantitation of time- and frequency-resolved optical spectra for the determination of tissue oxygenation. *Anal Biochem*. 1991;195(2):330-351. doi:10.1016/0003-2697(91)90339-U.
- [11] Chance B, Cope M, Gratton E, Ramanujam N, Tromberg BJ. Phase measurement of light absorption and scatter in human tissue. *Rev Sci Instrum*. 1998;69(10):3457-3481. doi:10.1063/1.1149123.
- [12] Farrell TJ, Patterson MS, Wilson B. A diffusion theory model of spatially resolved, steady-state diffuse reflectance for the noninvasive determination of tissue optical properties in vivo. *Med Phys.* 2005;19(4):879-888. doi:10.1118/1.596777.
- [13] Fantini S, Franceschini MA, Fishkin JB, Barbieri B, Gratton E. Quantitative determination of the absorption spectra of chromophores in strongly scattering media: a light-emitting-diode based technique. *Appl Opt.* 1994;33(22):5204. doi:10.1364/AO.33.005204.
- [14] Fishkin JB, Gratton E. Propagation of photon-density waves in strongly scattering media containing an absorbing semi-infinite plane bounded by a straight edge. *J Opt Soc Am A*. 1993;10(1):127-140. doi:10.1364/JOSAA.10.000127.